Talanta 198 (2019) 111–117

Contents lists available at ScienceDirect

Talanta

journal homepage: www.elsevier.com/locate/talanta

Detection of KRAS G12D point mutation level by anchor-like DNA electrochemical biosensor

Ni Zeng[a,b], Juan Xiang[a,b,*]

[a] Hunan Provincial Key Laboratory of Efficient and Clean Utilization of Manganese Resources, Central South University, Changsha 410083, Hunan, PR China
[b] College of Chemistry and Chemical Engineering, Central South University, Changsha 410083, Hunan, PR China

ARTICLE INFO

Keywords:
KRAS point mutation
Electrochemical biosensor
Formamide (FA)
Dual-functional detection

ABSTRACT

KRAS G12D point mutation plays an important role in the incidence of non-small-cell lung cancer (NSCLC) as well as colorectal cancer, pancreatic cancer and breast cancer. Here, we developed a novel anchor-like DNA (alDNA) electrochemical sensor for the detection of KRAS point mutation level (the concentration ratio of the specific KRAS point mutant DNA (M-DNA) to the total DNA (t-DNA) of both mutant and wild-type DNAs carrying the same allele). Compared to those conventional ligation-based DNA sensors, the proposed alDNA sensor achieved the one-step capture of both wild-type and mutant DNA, and the subsequent detection on one chip, which effectively decreased systematic errors from the uncertain differences on the interfacial structural and microenvironmental changes, improved the detection accuracy. Also, with the usage of formamide-NaCl solution, the whole detection process including the denaturation of double-stranded DNA was performed under mild temperature conditions (~40 °C). It greatly decreased the cost and improved the reproducibility and feasibility of the method. Based on it, the linear correlations with the logarithm of concentration in wide range from 0.1 pM to 10 nM for t-DNA and from 100 pM to 10 nM for M-DNA were achieved, respectively. The analysis of t-DNA- and M-DNA-spiked human serum samples revealed the high accuracy of the method. This alDNA sensor is convenient, low-cost and time-saving, with broad dynamic range, high sensitivity and selectivity. It can meet the demands of the clinical detection on the KRAS point mutation level in blood samples, which means significant for the earlier NSCLC diagnosis, individualized treatment, and therapeutic efficacy evaluation.

1. Introduction

DNA point mutations can change the amino acid sequence of downstream proteins and lead to various diseases such as cancers [1]. Analyzing the genotype and the mutation of specific gene means significant for the early diagnosis, individualized treatment, and therapeutic efficacy evaluation of cancers [2,3]. Lung cancer is one of the most common incident cancer with the highest cancer death rate [4–6]. The principle lung cancer is non-small-cell lung cancer (NSCLC) which usually harbors KRAS mutations [7,8]. The G12D transition (G→A) is one of the most common mutations in NSCLC patients including never smokers [9]. In addition, it also associates with many other kinds of cancers such as colorectal cancer [10], pancreatic cancer [11] and breast cancer [12]. Therefore, accurate detection of KRAS G12D point mutation has attracted great concerns in recent decade years. Many technologies including Sanger sequencing [13], quantitative polymerase chain reaction (qPCR) [14], next-generation sequencing (NGS) [15], and digital polymerase chain reaction (dPCR) [16] have been widely used in the clinical diagnosis of KRAS mutation in lung cancer. These technologies can be used to quantify DNA and figure out the genotype, but most of them are time-cost and expensive. To achieve rapid and more economical detections, various sensing strategies such as molecular beacon [17] , enzymatic cleavage [18], and ligation [19] have been developed and generally cooperated with fluorescence [19], colorimetry [20], and SERS [21]. Despite most of these techniques have achieved time-saving and reproducible detection for DNA point mutations, they are still facing challenges in clinic applications.

Mutated DNA could exist in health people and display significant concentration changes in patients with the progress or treatment of the diseases. Recently, the Wellcome Trust Sanger Institute revealed that almost everyone inherits dozens of DNA mutations from their parents [22]. For middle-age healthy people, it is inevitable that cells carrying DNA mutations exist in some organs [23]. As a result, some important cancer-related DNAs have been widely uncovered in normal tissues and

* Corresponding author at: Hunan Provincial Key Laboratory of Efficient and Clean Utilization of Manganese Resources, Central South University, Changsha 410083, Hunan, PR China.
E-mail address: xiangj@csu.edu.cn (J. Xiang).

https://doi.org/10.1016/j.talanta.2019.01.105
Received 29 November 2018; Received in revised form 25 January 2019; Accepted 29 January 2019
Available online 31 January 2019
0039-9140/

peripheral blood [24]. Since present DNA detections mainly depend on the polymerase chain reaction, these low-abundant cancer-related DNAs may greatly disturb the DNA detection and decrease the accuracy of cancer diagnosis. In another hand, even if the mutated DNA can reflect the process of tumor load, metastasis, and drug resistance, both the plasma free DNA and mutated DNA significantly change with the progress or treatment of cancer. Therefore, compared to the KRAS G12D point mutation concentration, its mutation level (M-DNA/t-DNA) which was defined as the concentration ratio of the KRAS G12D mutation (M-DNA) to the total KRAS (t-DNA, including mutant DNA and wild-type DNA), should be a more effective index for the earlier diagnosis, individualized treatment, and therapeutic efficacy evaluation of cancer.

According to traditional gene techniques, to achieve the KRAS G12D point mutation level, dual-channel method and instrumental for double-signal detection is necessary. However, dual-channel techniques inevitably encounter uncertain background differences which induce poor reproducibility, robustness, and accuracy [25–29]. The situation is aggravated when these biomarkers display large concentration differences. It requires the simultaneous detection of two forms with not only high sensitivity but also the ability to tune the detection range with convenient operation. Ultra-sensitive assays with broad detection range can enable these detections, but they mostly rely on skilled operators, complicated equipment and detection process [30]. Herein, to meet these challenges, we developed a novel anchor-like DNA (alDNA) electrochemical sensor to evaluate the KRAS G12D point mutation level. The alDNA was formed by the partially hybridization between a thiolated DNA and a methylene blue (MB) -labeled DNA. The unmatched part in the alDNA cooperated to capture and quantify the t-DNA. After treating the t-DNA covered alDNA sensor with denaturation process, the M-DNA could be accurately detected. The dynamic ranges of our method for t-DNA and M-DNA were 0.1 pM to 10 nM and 100 pM to 10 nM, respectively. This convenient, low-cost and time-saving method displayed broad dynamic range and high sensitivity, which meet the demands of the clinical detection on the KRAS G12D point mutation level in peripheral blood samples, meaning significant for the earlier NSCLC diagnosis, individualized treatment, and therapeutic efficacy evaluation.

2. Experimental section

2.1. Reagents

All oligonucleotides listed in Table 1 were purchased from Shanghai Sangon Biotechnology Co., Ltd. (Shanghai, China). All the blood samples were obtained from Xiangya Hospital Central South University (Changsha, China). NaCl, KCl, $MgCl_2$, $CaCl_2$, Tris(hydroxymethyl) aminomethane (Tris), Tris-HCl, and 6-Mercaptohexanol (MCH, 97%) were purchased from Sigma-Aldrich (Shanghai, China). Ethanol (99.7%) was purchased from Aladdin Industrial Co., Ltd. (Shanghai, China). EDTA (≥98.5%) and formamide (FA) (> 99%) were obtained from Shanghai Sangon Biotechnology Co., Ltd. (Shanghai, China). *E. coli* DNA ligase was purchased from Takara Biotechnology Co., Ltd. (Dalian, China), along with the 10-fold concentrated ligase buffer containing 300 mM Tris-HCl (pH 8.0), 40 mM $MgCl_2$, 100 mM $(NH_4)_2SO_4$, 12 mM EDTA, 1 mM nicotinamide adenine nucleotide (NAD), and 0.05% bovine serum albumin (BSA). All other chemicals were of analytical-grade purity and used without further purification. Deionized water (18.2 MΩ cm, Millipore M-Q System Inc., Milford, MA, USA) was used for all experiments.

2.2. Instruments

All the electrochemical impedance spectroscopy (EIS) and cyclic voltammetry (CV) measurements were conducted with a Gamry Reference 600 electrochemical workstation (Gamry Instruments Co., Ltd., Warminster, PA, U.S.A.). Square wave voltammetry (SWV) was conducted with a CHI832b electrochemical workstation (CH Instruments Ins., Shanghai, China), and the parameters were referred to our previous work [31]. A conventional three-electrode system was employed, with a platinum wire as the auxiliary electrode and an Ag/AgCl electrode filled with saturated KCl solution as the reference electrode. All the potentials were referred to the Ag/AgCl electrode. All the measurements were carried out at room temperature (ca. 25 °C).

2.3. Preparation of the alDNA sensor

The bare Au electrode (2 mm in diameter) was mechanically polished and electrochemically cleaned according to our previous work [31]. Two μM cDNA was mixed with equal volume of 2 μM pcDNA and incubated in a water bath at 37 °C for 2 h to form the alDNA. Then, 12 μL of the alDNA solution was dropped on the Au surface and incubated in the dark for 14 h. After rinsed with Tris-HCl and deionized water thoroughly, the electrode was immersed in 1 mM MCH solution for 1 h to block the unmodified spots and displace nonspecifically bound alDNA.

2.4. Electrochemical detection process

All SWV measurements were performed in 10 mM PBS. For the detection of t-DNA, 12 μL target solution was dropped onto the alDNA sensor surface, and incubated at 37 °C for 1 h. After thoroughly rinsing the sensor with deionized water, the t-DNA concentration was determined by SWV. Afterwards, 10 μL 2 U/μL of *E. coli* DNA ligase solution was added on the electrode and incubated at 37 °C for 2 h. After rinsed with Tris-HCl and deionized water, the electrode was immersed in the FA-NaCl solution (10 mM NaCl, 1 mM EDTA, 10 mM Tris and 50% v/v FA) and incubated at 40 °C for 30 min to denature the double-stranded DNA. After rinsing the electrode with 4 °C deionized water (to prevent the DNA from hybridization again), the M-DNA concentration was detected by SWV.

Table 1
Names and sequences of all the oligonucleotides used in this work.

Name	Sequence (5'→3')*	Length	T_M (°C)
cDNA	SH-$(CH_2)_6$-TTTTCAACTAGGCACTCTTGCCTACGCCA	29	63.7
pcDNA	P-TCAGCTCCAACTACCAGTTGA-MB	21	55.5
Wt-DNA	CTTGTGGTAGTTGGAGCTG G TGGCGTAGGCAAGAGTGCCT	40	70.0
MUt-DNA	CTTGTGGTAGTTGGAGCTG A TGGCGTAGGCAAGAGTGCCT	40	69.3

* Red color for sequences of alDNA's double-stranded part. Underlined sequences represent the matching segments in different DNAs.

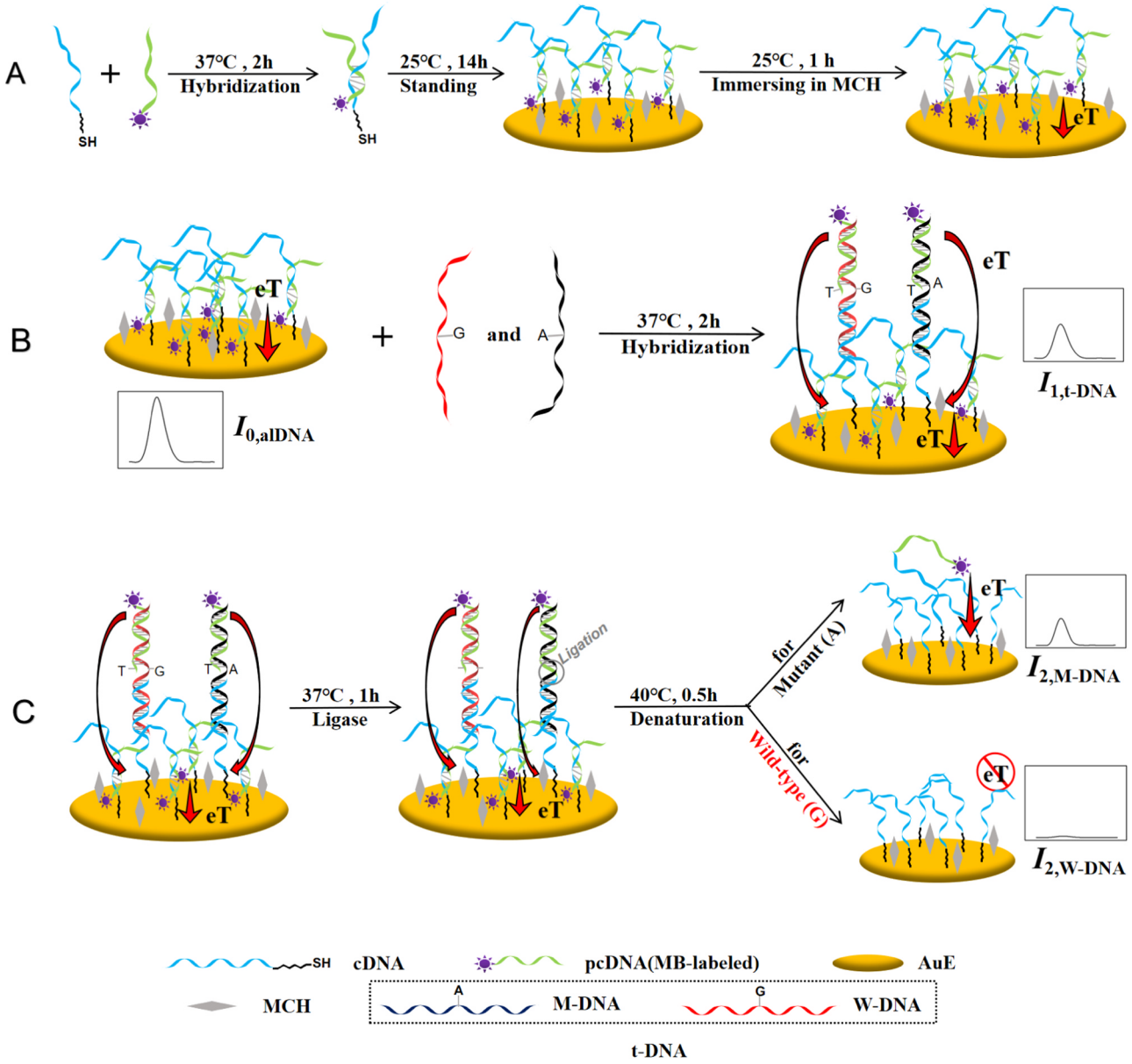

Scheme 1. Schematic representation of the formation of the alDNA sensing surface (A), and the detection mechanism of the t-DNA (B) and M-DNA(C).

2.5. Preparation of human serum sample

All the blood samples were obtained from Xiangya Hospital Central South University (Changsha, China). All of the protocols were reviewed by the Joint Ethics Committee of the Central South University Health Authority and performed in accordance with national guidelines. The blood sample was centrifugated at 2000 rpm for 15 min to get the blood serum. Then, the separated serum sample was treated with 100 kDa ultra-filtration membrane to filter some coexisting proteins with larger molecular weight in serum, reducing the interference from the non-specific adsorption of co-existing proteins on the practical detection. At last, the serum sample was stored at −80 °C for later use. Before the detection involving serum sample, the ultra-filtered serum sample was 10-fold diluted using phosphate buffer solution (pH 7.4).

3. Results and discussion

3.1. Design strategy

Scheme 1 depicts the preparation of the alDNA sensor and the detection mechanism of point mutation level. The alDNA is formed by the hybridization reaction between a thiolated DNA (cDNA) and a MB-labeled DNA (pcDNA). Six complementary base pairs between cDNA and pcDNA, acted as the anchor shrank, stabilize the anchor-like conformation of alDNA [32,33] with the electrochemical probe MB close to the electrode. The unmatched part in cDNA (including 20 bases) and the whole sequence in pcDNA, cooperates as a capture part for the target t-DNA (including W-DNA and M-DNA). Once the t-DNA is captured, the rigid duplex formed between the capture part and the t-DNA will unwind the hybridization on the alDNA shrank. pcDNA turns up and the electrochemical probe MB moves far away from the electrode. Then, the resulted current ($I_{1,t\text{-}DNA}$) can be employed for the quantitative detection of t-DNA. Afterwards, due to the complete base match between the capture part and the M-DNA, DNA ligase is used to link pcDNA onto cDNA. Subsequently, the sensor is incubated in a FA-NaCl solution at a mild temperature to unwind all the remained duplex forms. As a result, only linked pcDNA is kept on the electrode. The obtained current from MB (I_2) could be employed for the quantitative detection of M-DNA. The mutation level, defined as $c_{M\text{-}DNA}/c_{t\text{-}DNA}$, is achieved.

For the first time, the proposed alDNA sensor achieves the detection of DNA mutation level in one chip. Compared to those conventional ligation-based DNA sensors, the proposed alDNA sensor has several advantages. First, due to the close affinities to the capture part of alDNA, both W-DNA and M-DNA can be captured and detected in one step on one chip. Since the responses come from uniform interfacial structure, the uncertain differences on the interfacial structural and microenvironmental changes which usually appear in the traditional multi-channel detections, can be effectively eliminated. In addition, W-DNA and M-DNA are synchronously captured from one sample solution, which will effectively decrease systematic errors, improve the detection accuracy. Second, the unmatched part in cDNA and pcDNA, acted as the flock part on the alDNA, faces directly to the bulk solution, facilitating the capture of target molecules under extremely low concentrations. Third, with the usage of the FA-NaCl solution, the whole detection process including the denaturation of double-stranded DNA is performed under mild temperature conditions (~40 °C). It will greatly decrease the cost and improve the reproducibility and feasibility of the method.

3.2. Feasibility of the alDNA sensor

In order to investigate the feasibility of the designed strategy for t-DNA detection, the SWV responses of the alDNA sensor was detected before and after incubation with target DNA molecules. As shown in Fig. 1A, on the bare alDNA sensor, the peak current appears at −0.27 V, which is accordant with the electrochemical oxidation potential of MB, indicating the successful assembly of alDNA on the Au electrode. After incubation with 10 nM W-DNA or M-DNA solution, both obtained currents decrease (~36 nA for M-DNA and ~34 nA for W-DNA), confirming the effective capture of W-DNA and M-DNA on the alDNA sensor. The close current changes indicate the close affinities of both W-DNA and M-DNA to the alDNA. It ensures the co-capture of W-DNA and M-DNA in one step with slight competitive interference between two recognition events. Since the recognitions of two DNA forms occur on uniform interfacial structure, the uncertain interfacial structural and microenvironmental changes which usually appear in the traditional multi-channel detection, could be effectively eliminated.

Also, the feasibility of the designed strategy for M-DNA detections was investigated. As shown in Fig. 1B, after treated with DNA ligase and FA-NaCl solution, both alDNA/Au and W-DNA covered alDNA/Au (W-DNA/alDNA/Au) display slight electrochemical signals. It is attributed to the FA-NaCl-induced unwinding of double-strand DNA, and subsequent removing of pcDNA from the sensor. However, on M-DNA covered alDNA/Au (M-DNA/alDNA/Au), because of the complete base match between the capture part of alDNA and the M-DNA, DNA ligase effectively fixed the gap between cDNA and pcDNA. As a result, the pcDNA was kept on the sensor even all the double-strand DNAs were unwound and the M-DNA was removed. Then, a significant peak current proportional to the M-DNA concentration was obtained, as curve b in Fig. 1B.

EIS was used to further confirm the interface changes during the alDNA fabrication and its application on t-DNA and M-DNA detections. In Fig. 2, all the Nyquist plots of EIS consist a semicircle whose diameter is proportional to the interfacial electron transfer resistance R_{et}, and a long tail denoting diffusion of the redox species $[Fe(CN)_6]^{3-/4-}$. The bare Au electrode displays a tiny semicircle diameter (curve a), indicating a very fast electron transfer process. With the immobilization of alDNA and MCH, the interfacial electron transfer was blocked and the semicircle diameter obviously increased (curve b). After alDNA sensor hybridized with M-DNA or W-DNA, the R_{et} further increased (curve c). It can be attributed to the double-stranded DNA with negatively charged phosphate backbone greatly repelling the $[Fe(CN)_6]^{3-/4-}$ from the electrode surface. After treated with denaturation process, the R_{et} decreased dramatically on both W-DNA/alDNA/Au and M-DNA/alDNA/Au (curve d), which is accordant with the removal of target DNA from the electrode. Moreover, due to the additional removal of pcDNA, the R_{et} was smaller on the W-DNA/alDNA/Au.

3.3. Optimization of the detection conditions

Since Wallace rule was announced and became the most common equation for melting temperature (T_M) prediction [34], high temperature has been generally adopted to denature the DNA duplex. Usually, a reaction temperature above 90 °C is necessary for effective denaturation. However, such high temperature could also induce the rearrange of immobilized molecules, significantly reducing the detection reproducibility. In this paper, we successfully avoid the high temperature process with the usage of FA-NaCl solution. FA can compete efficiently with the H-bonds between Watson-rick base pairs and lower the T_M of DNA by about 0.60 °C/% FA (v/v) in solution [35]. In addition, according to Debye–Hückel electron shielding theory [36], the hybridization of DNA recedes logarithmically with decreased ionic strength. Based on these, we systematically investigated the effect of the FA concentration and the ionic strength on the DNA denaturation at 40 °C, a temperature close to the physiological condition. The denaturation efficiency was evaluated with $I_{2,W\text{-}DNA}$, which corresponded to the SWV response of the W-DNA/alDNA/Au after treated with ligation and denaturation process.

Obviously, the FA content significantly affects the denaturation effect. As shown in 3 A, with the FA content up to 50% v/v, the $I_{2,W\text{-}DNA}$ value decreased to its lowest level of ~4.9 nA. This value is close to the

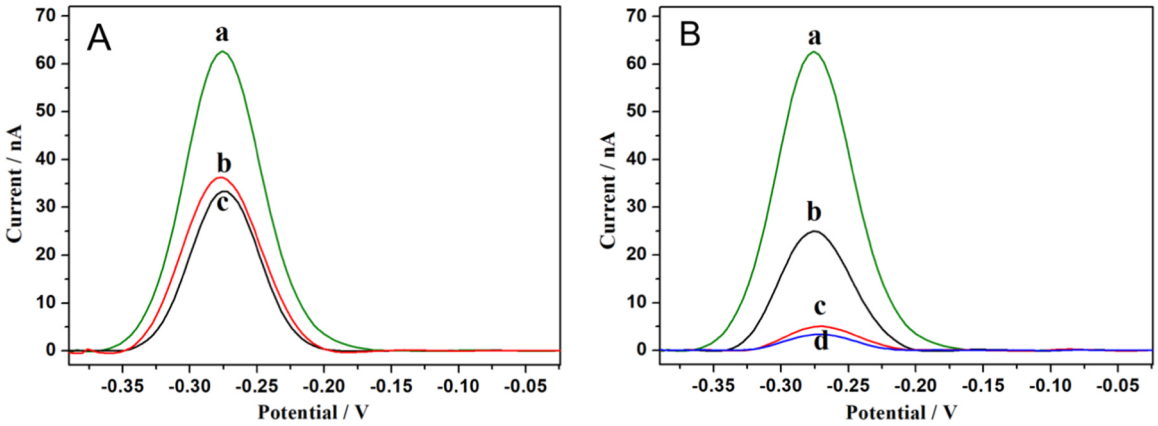

Fig. 1. Feasibilities of the alDNA sensing strategy for the t-DNA (A) and M-DNA (B) detections. (A) SWV responses of alDNA/Au (**a**), and the electrode treated with 10 nM M-DNA (**b**) or 10 nM W-DNA (**c**) in 10 mM PBS (pH 7.4). (B) SWV responses of denatured M-DNA/alDNA/Au (**b**), W-DNA/alDNA/Au (**c**), and alDNA/Au (**d**). The responses of bare alDNA/Au were displayed as curve a.

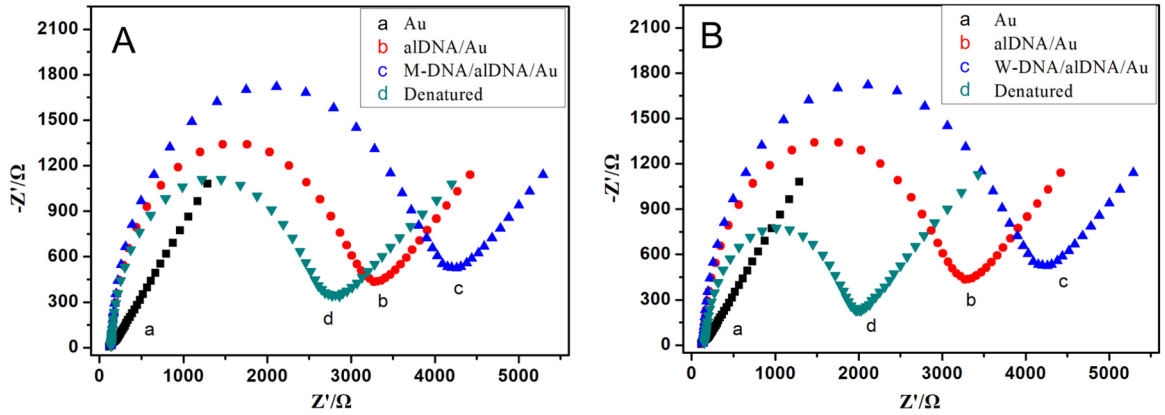

Fig. 2. Electrochemical impedance spectra of the different electrodes treated with M-DNA (A) or W-DNA (B) in 0.1 M KCl aqueous solution containing 5 mM $[Fe(CN)_6]^{3-/4-}$ as redox species.

SWV response of bare alDNA after denaturation (~4.7 nA in Fig. 1B), which corresponds to non-specific adsorption of free pcDNA on the electrode. Therefore, the optimal FA content is 50% v/v, which ensures the completely denaturation of the double-stranded DNA. Fig. 3B displays the slightly effect of NaCl concentration on the DNA denaturation. To ensure the stability of the sensor, 10 mM NaCl was used. Additionally, to achieve fast detection, the optimal denaturation time was investigated. The $I_{2,W\text{-}DNA}$ value decreased as the denaturation time increased from 0 to 30 min and then leveled off (Fig. 3C). Therefore, for this sensing system, 30 min is the optimal denaturation time. Compared to traditional high-temperature denaturation process, our method greatly simplified the operation and shortened the detection time, facilitating its application on the time-saving and low-cost assay.

3.4. Quantification detection of specific KRAS DNA and its G12D point mutation

Fig. 4A displayed the SWV responses of the alDNA sensor after treated with W-DNA or M-DNA, respectively. Obviously, with the $c_{W\text{-}DNA}$ and $c_{M\text{-}DNA}$ increasing, the corresponding SWV responses (defined as $I_{1,W\text{-}DNA}$ and $I_{1,M\text{-}DNA}$) decreased gradually. To reduce the systematic errors, all the peak currents were normalized (N_I) by compared with the initial peak current value corresponding to the bare alDNA ($I_{0,alDNA}$), and inserted in Fig. 4A. As expected, both calibration curves displayed

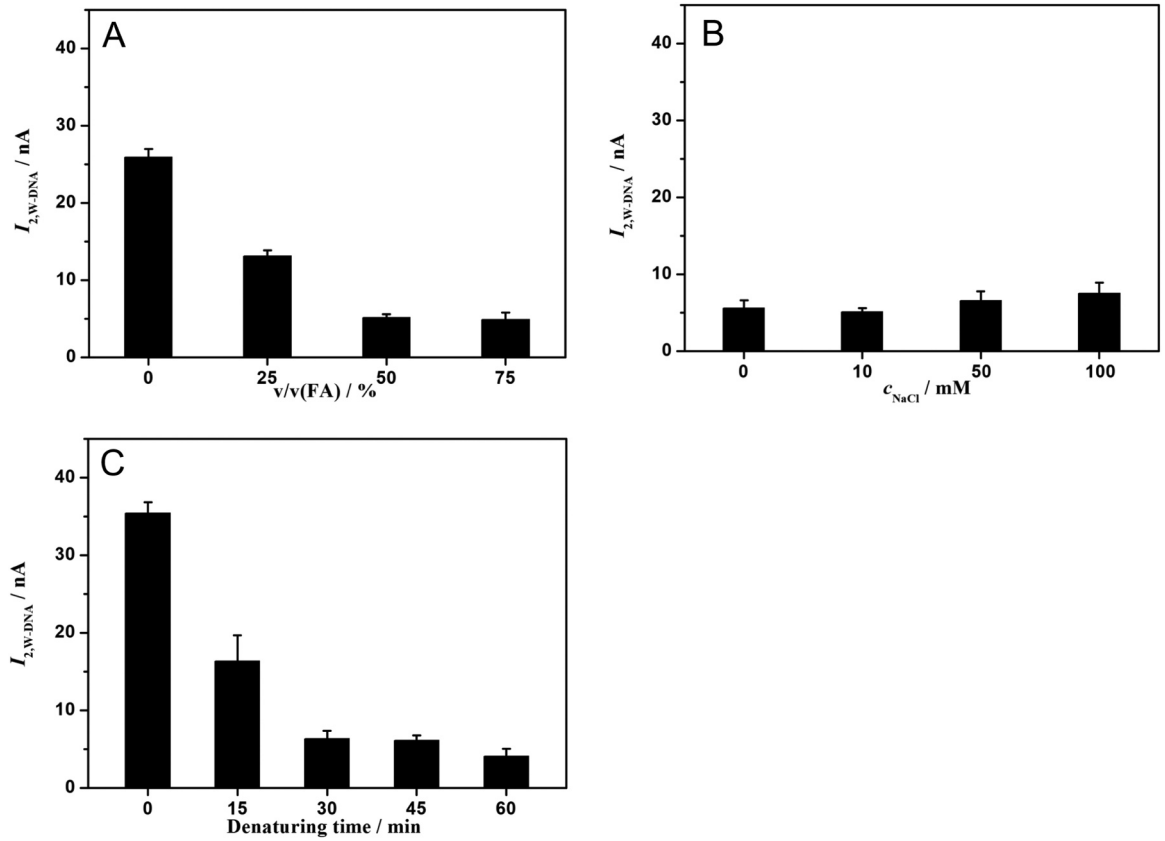

Fig. 3. Optimization of experimental conditions. (A) Dependence of $I_{2,W\text{-}DNA}$ on the volume percentage of FA in the denaturation solution (FA + 10 mM NaCl + 1 mM EDTA + 10 mM Tris (pH 7.0)). (B) Dependence of $I_{2,W\text{-}DNA}$ on the concentration of NaCl in the denaturation solution (NaCl + 50% FA + 1 mM EDTA + 10 mM Tris (pH 7.0)). (C) Dependence of $I_{2,W\text{-}DNA}$ on the denaturation time in FA-NaCl solution (50% FA + 10 mM NaCl + 1 mM EDTA + 10 mM Tris (pH 7.0)). All the current was detected on 10 nM W-DNA modified alDNA sensor in 10 mM PBS (pH 7.4). Error bars represent the RSD from three independent experiments.

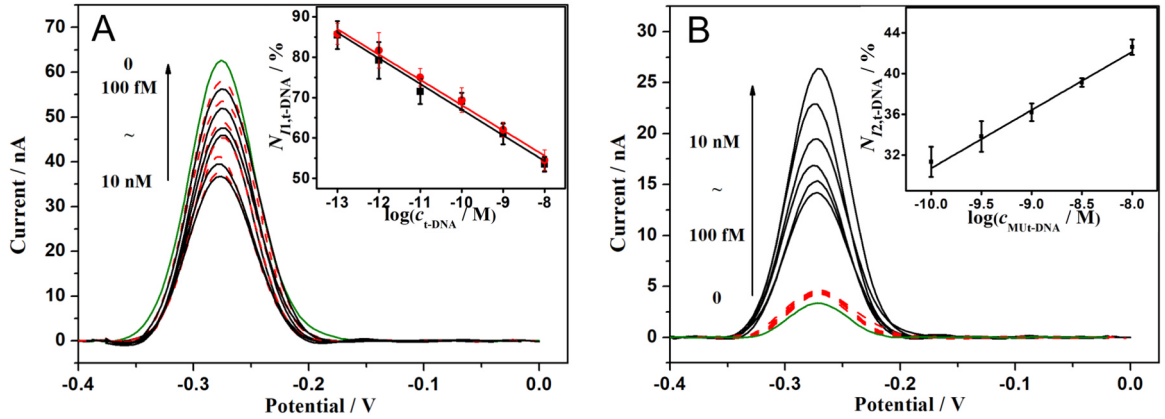

Fig. 4. Detections of the t-DNA and M-DNA. (A) SWV curves of the alDNA after incubated with M-DNA (black solid curves) or W-DNA (red dashed curves) under different concentrations. Inserted is the dependence of $N_{I1,t\text{-}DNA}$ on the concentration of M-DNA (black solid curves) or W-DNA (red dashed curves). (B) SWV curves of the M-DNA/alDNA (black solid curves) or W-DNA/alDNA (red dashed curves) after treated with *E. coli* DNA ligase and FA-NaCl solution. Inserted is the dependence of $N_{I2,M\text{-}DNA}$ on log$c_{M\text{-}DNA}$. Error bars represent the RSD from three independent determinations. (For interpretation of the references to color in this figure legend, the reader is referred to the web version of this article.)

Table 2
Recoveries of the t-DNA detection in 10-fold-diluted human blood serum samples.

Sample	Added (nM)	Found (nM)	Recovery (%)	RSD (%)
1	0.1 (MUt-DNA)	0.093 ± 0.006	93	6
2	1 (MUt-DNA)	1.005 ± 0.074	101	7
3	0.1 (Wt-DNA)	0.099 ± 0.003	99	3
4	1 (Wt-DNA)	1.087 ± 0.116	109	12
5	1 (50%MUt-DNA + 50%Wt-DNA)	1.168 ± 0.136	117	12

Table 3
Recoveries of the G12D M-DNA detection in 10-fold-diluted human blood serum samples.

Sample	Added (nM)	Found (nM)	Recovery (%)	RSD (%)
1	0.1	0.091 ± 0.012	91	12
2	0.5	0.503 ± 0.015	101	3
3	1	1.043 ± 0.031	104	3

similar feature, including good linear relationship with respect to the analyte concentration ranging from 0.1 pM to 10 nM and close linear equations ($N_{I1,W\text{-}DNA} = -6.2633 \log c_{W\text{-}DNA} + 5.5161$ ($R = 0.9917$); $N_{I1,M\text{-}DNA} = -6.3623 \log c_{M\text{-}DNA} + 3.4076$ ($R = 0.9974$)). Based on it, an average linear relationship with respect to the t-DNA concentration ($c_{t\text{-}DNA}$) ranging from 0.1 pM to 10 nM ($N_{I1,t\text{-}DNA} = -6.3128 \log c_{t\text{-}DNA} + 4.4619$) was obtained, which can be used for the quantitative detection of t-DNA.

After treating the M-DNA covered alDNA sensor (M-DNA/alDNA) with DNA ligase and FA-NaCl solution, the M-DNA concentrations were directed detected by the SWV responses. As displayed in Fig. 4B, with the $c_{M\text{-}DNA}$ increasing, the corresponding SWV responses (defined as $I_{2,M\text{-}DNA}$) increased gradually. On contrary, both bare and W-DNA covered alDNA displayed small residual currents after denaturation process, which should be ascribed to the non-specific adsorption of pcDNA. It confirmed that both W-DNA and unreacted alDNA have slight disturbance on the M-DNA detection. To reduce the systematic errors, after subtract the residual current, all the peak currents from M-DNA/alDNA were normalized ($N_{I2,M\text{-}DNA}$) by compared with $I_{0,alDNA}$, and inserted in Fig. 4B. A good linear relationship of $N_{I2,M\text{-}DNA} = 5.7213 \log c_{M\text{-}DNA} + 87.9224$ ($R = 0.9850$) with the dynamic region of $c_{M\text{-}DNA}$ from 100 pM to 10 nM was obtained for the quantitative detection of M-DNA. The M-DNA concentration in peripheral blood from patients with advanced tumors approximately ranges from 10^{-10} to 10^{-8} M [37,38]. Therefore, this proposed electrochemical method can meet the demands of the clinical M-DNA level detection in peripheral blood for the NSCLC diagnosis and therapeutic efficacy evaluation.

Finally, to assess its analytical application in real blood samples, the alDNA sensor was employed to measure M-DNA and its t-DNA in 10-fold diluted human blood serum samples. The diluted human serum samples spiked with W-DNA and M-DNA at different concentrations were investigated. All recoveries listed in Tables 2 and 3 confirm that the alDNA sensor can achieve good performance for both t-DNA and M-DNA detection in the serum samples, with an RSD of 3–12%. Therefore, the developed method possesses high accuracy and is acceptable for the practical detection.

4. Conclusions

This study developed a novel alDNA electrochemical sensor for the detection of KRAS G12D point mutation level. Compared to those conventional ligation-based DNA sensors, the proposed alDNA sensor achieved the one-step capture of both wild-type and mutant DNAs carrying the same allele, and the subsequent detection on one chip. It effectively decreased systematic errors from the uncertain differences on the interfacial structural and microenvironmental changes, improving the detection accuracy. Also, with the usage of FA-NaCl solution, the whole detection process including the denaturation of double-stranded DNA was performed under mild temperature conditions. It greatly decreased the cost and improved the reproducibility and feasibility of the method. Based on it, the linear correlations with the logarithm of concentration in wide range from 0.1 pM to 10 nM for t-DNA and from 100 pM to 10 nM for M-DNA were achieved, respectively. The analysis of t-DNA-spiked human serum samples revealed the high accuracy of the method. This alDNA sensor is convenient, low-cost and time-saving, with broad dynamic range, high sensitivity and selectivity. It can meet the demands of the clinical detection on the KRAS point mutation level in blood samples, which means significant for the earlier NSCLC diagnosis, individualized treatment, and therapeutic efficacy evaluation.

Acknowledgements

This work was financially supported by the National Natural Science Foundation of China (21573290), and the Open Research Fund of State Key Laboratory of Physical Chemistry of Solid Surface (201814).

References

[1] V. Wiest, I. Eisenbarth, C. Schmegner, W. Krone, G. Assum, Somatic NF1 mutation spectra in a family with neurofibromatosis type 1: toward a theory of genetic modifiers, Hum. Mutat. 22 (6) (2003) 423–427, https://doi.org/10.1002/humu.10272.

[2] C.C. Wu, H.Y. Hsu, H.P. Liu, J. Chang, Y.T. Chen, W.Y. Hsieh, J.J. Hsieh, M.S. Hsieh, Y.R. Chen, S.F. Huang, Reversed mutation rates of KRAS and EGFR genes in adenocarcinoma of the lung in Taiwan and their implications, Cancer 113 (11) (2010) 3199–3208, https://doi.org/10.1002/cncr.23925.

[3] J.L. Guan, W.Z. Zhong, S.J. An, J.J. Yang, J. Su, Z.H. Chen, H.H. Yan, Z.Y. Chen, Z.M. Huang, X.C. Zhang, Q. Nie, Y.L. Wu, KRAS mutation in patients with lung cancer: a predictor for poor prognosis but not for EGFR-TKIs or chemotherapy, Ann. Surg. Oncol. 20 (4) (2013) 1381–1388, https://doi.org/10.1245/s10434-012-2754-z.

[4] N. Tsuchida, T. Ryder, E. Ohtsubo, Nucleotide sequence of the oncogene encoding the p21 transforming protein of Kirsten murine sarcoma virus, Science 217 (4563) (1982) 937, https://doi.org/10.1126/science.6287573.

[5] O. Kranenburg, The KRAS oncogene: past, present, and future, BBA-Rev. Cancer 1756 (2) (2005) 81–82, https://doi.org/10.1016/j.bbcan.2005.10.001.

[6] Global Burden of Disease Cancer, C. Fitzmaurice, Global, regional, and national cancer incidence, mortality, years of life lost, years lived with disability, and disability-adjusted life-years for 29 cancer groups, 1990 to 2016: a systematic analysis for the global burden of disease study, JAMA Oncol. (2018), https://doi.org/10.1001/jamaoncol.2018.2706.

[7] S. Rodenhuis, M.L. Wetering, W.J. Mooi, S.G. Evers, N. Zandwijk, Van, J.L. Bos, Mutational activation of the K-ras oncogene: a possible pathogenetic factor in adenocarcinoma of the lung, N. Engl. J. Med. 317 (15) (1987) 929–935, https://doi.org/10.1056/NEJM198710083171504.

[8] S. Forbes, J. Clements, E. Dawson, S. Bamford, T. Webb, A. Dogan, A. Flanagan, J. Teague, R. Wooster, P.A. Futreal, M.R. Stratton, Cosmic 2005, Br. J. Cancer 94 (2) (2006) 318–322, https://doi.org/10.1038/sj.bjc.6602928.

[9] G.J. Riely, M.G. Kris, D. Rosenbaum, J. Marks, A. Li, D.A. Chitale, K. Nafa, E.R. Riedel, M. Hsu, W. Pao, V.A. Miller, M. Ladanyi, Frequency and distinctive spectrum of KRAS mutations in never smokers with lung adenocarcinoma, Clin. Cancer Res. 14 (18) (2008) 5731–5734, https://doi.org/10.1158/1078-0432.CCR-08-0646.

[10] A. Lievre, J.B. Bachet, V. Boige, A. Cayre, D. Le Corre, E. Buc, M. Ychou, O. Bouche, B. Landi, C. Louvet, T. Andre, F. Bibeau, M.D. Diebold, P. Rougier, M. Ducreux, G. Tomasic, J.F. Emile, F. Penault-Llorca, P. Laurent-Puig, KRAS mutations as an independent prognostic factor in patients with advanced colorectal cancer treated with cetuximab, J. Clin. Oncol. 26 (3) (2008) 374–379, https://doi.org/10.1200/JCO.2007.12.5906.

[11] K. Yoshikawa, E. Tanabe, A. Shibata, S. Inoue, M. Kitayoshi, S. Okimoto, N. Fukushima, T. Tsujiuchi, Involvement of oncogenic K-ras on cell migration stimulated by lysophosphatidic acid receptor-2 in pancreatic cancer cells, Exp. Cell Res. 319 (3) (2013) 105–112, https://doi.org/10.1016/j.yexcr.2012.09.014.

[12] J.M. Balko, I.A. Mayer, M.E. Sanders, T.W. Miller, M.G. Kuba, I.M. Meszoely, N. Wagle, L.A. Garraway, C.L. Arteaga, Discordant cellular response to presurgical letrozole in bilateral synchronous ER + breast cancers with a KRAS mutation or FGFR1 gene amplification, Mol. Cancer Ther. 11 (10) (2012) 2301–2305, https://doi.org/10.1158/1535-7163.MCT-12-0511.

[13] F. Sanger, Determination of nucleotide sequences in DNA, Biosci. Rep. 214 (4526) (1981) 1205–1210, https://doi.org/10.1007/BF01115145.

[14] K.L. Spindler, N. Pallisgaard, R.F. Andersen, I. Brandslund, A. Jakobsen, Circulating free DNA as biomarker and source for mutation detection in metastatic colorectal cancer, PLoS One 10 (4) (2015) 0108247, https://doi.org/10.1371/journal.pone.0108247.

[15] R.K. Patel, M. Jain, NGS QC Toolkit: a toolkit for quality control of next generation sequencing data, PLoS One 7 (2) (2012) e30619, https://doi.org/10.1371/journal.pone.0030619.

[16] S. Dube, J. Qin, R. Ramakrishnan, Mathematical analysis of copy number variation in a DNA sample using digital PCR on a nanofluidic device, PLoS One 3 (8) (2008) e2876, https://doi.org/10.1371/journal.pone.0002876.

[17] A. Latorre, C. Posch, Y. Garcimartin, S. Ortiz-Urda, A. Somoza, Single-point mutation detection in RNA extracts using gold nanoparticles modified with hydrophobic molecular beacon-like structures, Chem. Commun. 50 (23) (2014) 3018–3020, https://doi.org/10.1039/c3cc47862a.

[18] M. Olivier, The invader assay for SNP genotyping, Mutat. Res.-Fund. Mol. Mech. 573 (1–2) (2005) 103–110, https://doi.org/10.1016/j.mrfmmm.2004.08.016.

[19] Y. Song, Y. Zhang, T.H. Wang, Single quantum dot analysis enables multiplexed point mutation detection by gap ligase chain reaction, Small 9 (7) (2013) 1096–1105, https://doi.org/10.1002/smll.201202242.

[20] J.S. Li, X. Chu, Y.L. Liu, J.H. Jiang, Z.M. He, Z.W. Zhang, G.L. Shen, R.Q. Yu, A colorimetric method for point mutation detection using high-fidelity DNA ligase, Nucleic Acids Res. 33 (19) (2005) e168, https://doi.org/10.1093/nar/gni163.

[21] S. Kim, S.N. Jeong, S. Bae, H. Chung, S.Y. Yoo, Sensitive surface enhanced raman scattering-based detection of a BIGH3 point mutation associated with Avellino corneal dystrophy, Anal. Chem. 88 (23) (2016) 11288–11292, https://doi.org/10.1021/acs.analchem.6b03320.

[22] D.F. Conrad, J.E.M. Keebler, M.A. DePristo, S.J. Lindsay, Z. Yujun, C. Ferran, I. Youssef, C.L. Hartl, T. Carlos, K.V. Garimella, Variation in genome-wide mutation rates within and between human families, Nat. Genet. 43 (7) (2011) 712–714, https://doi.org/10.1038/ng.862.

[23] I. Martincorena, J.C. Fowler, A. Wabik, A.R.J. Lawson, F. Abascal, M.W.J. Hall, A. Cagan, K. Murai, K. Mahbubani, M.R. Stratton, R.C. Fitzgerald, P.A. Handford, P.J. Campbell, K.S. Parsy, P.H. Jones, Somatic mutant clones colonize the human esophagus with age, Science (2018) eaau3879, https://doi.org/10.1126/science.aau3879.

[24] J.D. Krimmel, M.W. Schmitt, M.I. Harrell, K.J. Agnew, S.R. Kennedy, M.J. Emond, L.A. Loeb, E.M. Swisher, R.A. Risques, Ultra-deep sequencing detects ovarian cancer cells in peritoneal fluid and reveals somatic TP53 mutations in noncancerous tissues, PNAS 113 (21) (2016) 6005–6010, https://doi.org/10.1073/pnas.1601311113.

[25] D.S. Gembitsky, K. Lawlor, A. Jacovina, M. Yaneva, P. Tempst, A prototype antibody microarray platform to monitor changes in protein tyrosine phosphorylation, Mol. Cell. Proteom. 3 (11) (2004) 1102–1118, https://doi.org/10.1074/mcp.M400075-MCP200.

[26] L. Pan, A. Iliuk, S. Yu, R.L. Geahlen, W.A. Tao, Multiplexed quantitation of protein expression and phosphorylation based on functionalized soluble nanopolymers, J. Am. Chem. Soc. 134 (44) (2012) 18201–18204, https://doi.org/10.1021/ja308453m.

[27] M. Swirski, J.S. Miners, R.D. Silva, T. Lashley, H. Ling, J. Holton, T. Revesz, S. Love, Evaluating the relationship between amyloid-β and α-synuclein phosphorylated at Ser129 in dementia with Lewy bodies and Parkinson's disease, Alzheimers Res. Ther. 6 (5–8) (2014) 77, https://doi.org/10.1186/s13195-014-0077-y.

[28] K.Q. Deng, C.X. Li, H.W. Huang, X.F. Li, Rolling circle amplification based on signal-enhanced electrochemical DNA sensor for ultrasensitive transcription factor detection, Sens. Actuators B-Chem. 238 (2017) 1302–1308, https://doi.org/10.1016/j.snb.2016.09.107.

[29] K.Q. Deng, X.Y. Liu, C.X. Li, H.W. Huang, Sensitive electrochemical sensing platform for microRNAs detection based on shortened multi-walled carbon nanotubes with high-loaded thionin, Biosens. Bioelectron. (2018), https://doi.org/10.1016/j.bios.2018.05.055.

[30] Y.K. Leng, K. Sun, X.Y. Chen, W.W. Li, Suspension arrays based on nanoparticle-encoded microspheres for high-throughput multiplexed detection, Chem. Soc. Rev. 44 (15) (2015) 5552–5595, https://doi.org/10.1039/C4CS00382A.

[31] M. Zhang, Q.Y. Zhai, L.P. Wan, C. Li, P. Yu, C.Y. Deng, J. Xiang, J.W. Yan, Electrochemical impedance spectroscopy for real-time detection of lipid membrane damage based on a porous self-assembly monolayer support, Anal. Chem. 90 (12) (2018) 7422–7427, https://doi.org/10.1021/acs.analchem.8b00884.

[32] A.J. Veloso, A.M. Chow, H.V. Ganesh, N. Li, D. Dhar, D.C. Wu, S. Mikhaylichenko, I.R. Brown, K. Kerman, Electrochemical immunosensors for effective evaluation of amyloid-beta modulators on oligomeric and fibrillar aggregation processes, Anal. Chem. 86 (10) (2014) 4901–4909, https://doi.org/10.1021/ac500424t.

[33] K.J. Breslauer, R. Frank, H. Blöcker, L.A. Marky, Predicting DNA duplex stability from the base sequence, PNAS 83 (11) (1986) 3746–3750, https://doi.org/10.1073/pnas.83.11.3746.

[34] R.B. Wallace, J. Shaffer, R.F. Murphy, J. Bonner, T. Hirose, K. Itakura, Hybridization of synthetic oligodeoxyribonucleotides to phi chi 174 DNA: the effect of single base pair mismatch, Nucleic Acids Res. 6 (11) (1979) 3543–3557, https://doi.org/10.1093/nar/6.11.3543.

[35] R.D. Blake, S.G. Delcourt, Thermodynamic effects of formamide on DNA stability, Nucleic Acids Res. 24 (11) (1996) 2095–2103, https://doi.org/10.1093/nar/24.11.2095.

[36] P. Debye, E. Hückel, De la theorie des electrolytes. I. Abaissement du point de congelation et phenomenes associes, Phys. Z. 24 (9) (1923) 185–206.

[37] C. Bettegowda, M. Sausen, R.J. Leary, I. Kinde, Y.X. Wang, N. Agrawal, B.R. Bartlett, H. Wang, B. Luber, R.M. Alani, Detection of circulating tumor DNA in early- and late-stage human malignancies, Sci. Transl. Med. 6 (224) (2014) 224ra24, https://doi.org/10.1126/scitranslmed.3007094.

[38] E. Gormally, P. Hainaut, E. Caboux, L. Airoldi, H. Autrup, C. Malaveille, A. Dunning, S. Garte, G. Matullo, K. Overvad, A. Tjonneland, Amount of DNA in plasma and cancer risk: a prospective study, Int. J. Cancer 111 (5) (2004) 746–749, https://doi.org/10.1002/ijc.20327.